Original Investigations

Comparison of Myocardial Perfusion Evaluation with Single Versus Dual-Energy CT and Effect of Beam-Hardening Artifacts

Patricia M. Carrascosa, MD, PhD, Ricardo C. Cury, MD, Alejandro Deviggiano, MD, Carlos Capunay, MD, Roxana Campisi, MD, Marina López de Munain, MD, Javier Vallejos, MD, Carlos Tajer, MD, Gaston A. Rodriguez-Granillo, MD, PhD

Rationale and objectives: We sought to explore the feasibility and diagnostic performance of dual-energy computed tomography (DECT) versus single-energy computed tomography (SECT) for the evaluation of myocardial perfusion in patients with intermediate to high likelihood of coronary artery disease.

Materials and Methods: The present prospective study involved patients with known or suspected coronary artery disease referred for myocardial perfusion imaging by single-photon emission computed tomography. Forty patients were included in the study protocol and scanned using DECT imaging (n = 20) or SECT imaging (n = 20). The same pharmacologic stress was used for DECT, SECT, and single-photon emission computed tomography scans.

Results: A total of 1360 left ventricular segments were evaluated by DECT and SECT. The contrast-to-noise ratio was similar between groups (DECT 8.8 $\pm$ 2.9 vs. SECT 7.7 $\pm$ 4.2; P = .22). The diagnostic performance of DECT was greater than that of SECT in identifying perfusion defects (area under the receiver operating characteristic curve of DECT 0.90 [0.86–0.94] vs SECT 0.80 [0.76–0.84]; P = .0004) and remained unaffected when including only segments affected by beam-hardening artifacts (area under the receiver operating characteristic curve = DECT 0.90 [0.84–0.96) vs. SECT 0.77 [0.69–0.84]; P = .007).

Conclusions: Our results suggest that myocardial perfusion by DECT imaging is feasible and might have improved diagnostic performance compared to SECT imaging for the assessment of myocardial CT perfusion. Furthermore, the diagnostic performance of DECT remained unaffected by the presence of beam-hardening artifacts.

Key Words: Computed tomography; spectral imaging; dypiridamole.

Until recently, coronary computed tomography angiography (CCTA) was limited to the anatomic assessment of coronary obstructions in patients with low to intermediate likelihood of coronary artery disease (CAD), whereas the functional significance of coronary stenoses remained outside its scope. Several studies have demonstrated the ability of CCTA to perform myocardium perfusion studies by using stress vasodilator agents (1–4). However, the clinical use of stress myocardium computed tomography (CT) perfusion is somewhat limited, mostly by technical issues including beam-hardening artifacts (BHAs), which are originated by the polychromatic nature of x-rays and the energy dependency of x-ray attenuation, and are related to a considerable myocardial signal density (SD) drop at regions in close proximity to highly attenuated structures, thus resembling perfusion defects (5).

With the advent of dual-energy computed tomography (DECT) imaging, BHAs could be reduced with the generation of synthesized monochromatic image reconstruction (6). We therefore sought to explore the feasibility and diagnostic performance of DECT versus single-energy computed tomography (SECT) for the evaluation of myocardial perfusion defects assessed by single-photon emission computed tomography (SPECT) in patients with intermediate to high likelihood of CAD. Furthermore, we sought to compare the diagnostic performance of DECT versus SECT among myocardial regions with high prevalence of BHAs.

Acad Radiol 2015; ■:1–9

From the Department of Cardiovascular Imaging, Diagnóstico Maipú, Av Maipú 1668, Vicente López, B1602ABQ Buenos Aires, Argentina (P.M.C., A.D., C.C., R.C., M.L.d.M., J.V., C.T., G.A.R.-G.); and Baptist Hospital of Miami, Miami, Florida; and Baptist Cardiac and Vascular Institute, Miami, Florida (R.C.C.). Received August 25, 2014; accepted December 23, 2014. We declare that Drs Patricia M. Carrascosa and Ricardo C. Cury are Consultants for GE. There are no competing interests related to the manuscript for any of the other authors. **Address correspondence to:** P.M.C. e-mail: patriciacarrascosa@diagnosticomaipu.com.ar

http://dx.doi.org/10.1016/j.acra.2014.12.019

METHODS

Study Population

The present work was a single-center, investigator driven, prospective study that involved patients with known or suspected CAD referred for myocardial perfusion imaging by SPECT. All patients included were older than 40 years, with stable heart rate and sinus rhythm, able to maintain a breath-hold for 15 seconds; without a history of contrast-related allergy, renal failure, or hemodynamic instability. Additional exclusion criteria comprised a body mass index greater than 32 kg/m^2, a history of previous myocardial infarction within the previous 30 days, percutaneous coronary revascularization within the previous 6 months, chronic heart failure, chronic obstructive pulmonary disease, high-degree atrioventricular block, or low estimated pretest probability of CAD.

Patients were advised to refrain from vasodilator medications for the previous 24 hours, as well as from smoking and caffeine beverages. Coronary risk factors and clinical status were recorded at the time of the CT scan, and clinical variables were defined as indicated by the Framingham Risk Score assessment. The estimated pretest likelihood of obstructive CAD was calculated using the Duke Clinical Score, which includes chest pain features, age, gender, and traditional risk factors. Patients were thus categorized as having low (1%–30%), intermediate (31%–70%), or high (71%–99%) estimated pretest likelihood of obstructive CAD (7,8).

Patients were sequentially scanned using 256-slice SECT (Brilliance ICT; Philips Healthcare, Cleveland, Ohio) or a CT scanner equipped with gemstone detectors with fast primary speed and low afterglow designed for DECT imaging (Discovery HD 750; GE Medical Systems, Milwaukee). The same pharmacologic stress was used for SECT, DECT, and SPECT scans. Dypiridamole (0.56 mg/kg) and iodinated contrast (iobitridol, Xenetix 350; Guerbet, Villepinte, France) were administrated using two independent antecubital intravenous lines. After dypiridamole infusion, aminophylline (1–2 mg/kg) was administrated intravenously to revert the vasodilator effect. The prespecified primary endpoint of the study was to compare the diagnostic performance of DECT versus SECT on a per segment basis using receiver operating characteristic (ROC) curve analyses. Furthermore, we sought to compare the diagnostic performance among segments commonly influenced by the presence of BHAs.

CT Perfusion Acquisition

In line with the primary end point of the study and the population involved (intermediate to high likelihood of CAD), stress myocardial perfusion imaging was performed first and rest imaging 30 minutes after stress imaging.

According to the guidelines of the Society of Cardiovascular Computed Tomography (SCCT) on radiation dose and dose-optimization strategies in cardiovascular CT (9), SECT studies were acquired using the following depending on the acquisition mode (retrospective or prospective) and body mass index.

Among retrospective (stress) acquisitions, maximum tube voltage was adjusted according to the body habitus (100 or 120 kV for patients with body mass index <30 kg/m^2 or greater, respectively). Likewise, tube current was adjusted according to the body habitus (800 or 1000 mAs for patients with body mass index <30 kg/m^2 or greater, respectively). Other scanner-related parameters were a collimation width of 0.625 mm, a slice interval of 0.625 mm, and a pitch of 0.18. Among prospective (rest) acquisitions, maximum tube voltage and current was adjusted according to the body habitus (100 or 120 kV for patients with body mass index <30 kg/m^2 or greater, respectively, and 200–250 mAs, respectively).

Dual-Energy CT

Stress myocardial perfusion imaging was performed after intravenous administration of dypiridamole using prospective electrocardiogram (ECG) gating including ~100 milliseconds of temporal padding aimed to comprise approximately 45%–75% of the R-R interval. DECT was performed by rapid switching (0.3–0.5 milliseconds) between low and high tube potentials (80–140 kV) from a single source, thereby allowing the reconstruction of low- and high-energy projections and generation of monochromatic image reconstructions with 10 keV increments from 40 to 140 keV. Iterative reconstruction was available for every energy level except from 40 and 50 keV (10). Three minutes after dypiridamole administration, a dual-phase protocol with 50–70 mL of iodinated contrast followed by a 30–40 mL saline flush was injected through an arm vein at an injection rate of 4.0–5.0 mL/s according to the vein access. A bolus tracking technique was used to synchronize the arrival of contrast at the level of the coronary arteries with the start of the scan, using a region of interest placed at the ascending aorta and a threshold of 120 Hounsfield units.

For rest-DECT imaging, patients with a heart rate of more than 65 bpm received 5 mg intravenous propranolol if needed to achieve a target heart rate of less than 60 bpm. Image acquisition at rest was performed using the same protocol as for stress-DECT, after sublingual administration of 2.5–5 mg of isosorbide dinitrate.

Single-Energy CT

Stress myocardial perfusion imaging with SECT was performed using retrospective ECG gating (because of the increased heart rate associated with pharmacologic stress) with dose pulsing, an algorithm designed to modulate the tube current according to the ECG during the spiral scan, after intravenous administration of dypiridamole. The same contrast injection protocol as for DECT was used. Iterative reconstruction was performed in all cases.

The rest SECT scan was performed using prospective ECG gating, without temporal padding, 30 minutes after stress-SECT. Patients with a heart rate of more than 65 bpm received 5 mg intravenous propranolol if needed to achieve a target heart rate of less than 60 bpm. Image acquisition was performed after administration of 2.5–5 mg of isosorbide dinitrate.

SPECT Myocardial Perfusion Imaging

At the time of the stress CT (SECT and DECT cohorts) perfusion scans, 2 minutes after dypiridamole administration and immediately before the CT scan, 10–15 mCi of technetium-99m-methoxy isobutyl isonitrile was administrated. Stress-SPECT image acquisition was performed 60 minutes after the administration of the radiotracer using a dual-head gamma camera over a 90° circular orbit (Millennium MG; GE Medical Systems). Data were acquired in a 128 × 128 matrix for 32 projections in a step and acquire format. Rest-SPECT image acquisition was completed within 24–48 hours after stress-SPECT, after administration of 10–15 mCi of technetium-99m-methoxy isobutyl isonitrile.

CT Perfusion Analysis

CT perfusion analysis was performed off-line on dedicated workstations, using a commercially available dedicated software tool (AW 4.6; GE Healthcare for DECT patients; and Comprehensive Cardiac Analysis, Brilliance Workspace; Philips Healthcare for SECT patients) by consensus of two experienced observers (P.C. and C.C.), blinded to the clinical data and to the SPECT results. CT images were analyzed at mid diastole using a smooth filter in axial planes and multiplanar reconstructions. Window and level settings were prespecified at 300 and 150, respectively, although observers were allowed to adjust these settings if deemed necessary. Short-axis views were obtained initially using 5–8 mm average multiplanar reconstructions from base to apex, with the full dataset available for the reader.

Evaluation of the presence of perfusion defects was carried out using 20 mm^2 intramyocardial regions of interest excluding a 1 mm subendocardial area to avoid BHAs or partial volume effects, according to the American Heart Association left ventricular 17-segment model (11). Myocardial perfusion defects were initially identified in a qualitative manner and subsequently defined as myocardium having a SD one standard deviation below the mean myocardial SD.

DECT images were evaluated using monochromatic data. Different energy levels from 40 to 100 keV were applied so as to confirm or to rule out the presence of a perfusion defect and to confirm a positive finding it was required to be identified at all the energetic levels. If the defect was present only at some energetic levels it was considered a BHA.

Using standardized regions of interest of 20 mm^2 localized at the interventricular septum over normally perfused myocardium, myocardial SD was determined (5).

The SD ratio was determined as previously described: myocardial SD/left ventricular blood pool SD (5). To assess image quality, we determined image noise and contrast-to-noise ratios. Image noise was derived from the standard deviation of the SD values (in Hounsfield units) within a large region of interest in the left ventricle. The contrast-to-noise ratio was defined as the difference between the mean density of the contrast-filled left ventricular chamber and the mean density of the left ventricular wall, which was divided by image noise. Image quality for DECT was assessed at 60–90 keV with the purpose of allowing the use of iterative reconstruction. Finally, to explore the impact of BHAs, we further evaluated the diagnostic performance of SECT and DECT including only segments more commonly affected by BHAs (AHA segments #5 [basal inferolateral], #13 [apical anterior], #14 [apical septal], #15 [apical inferior], and #16 [apical lateral]). BHAs were confirmed if the low attenuation myocardial segment was not associated with an underlying coronary artery stenosis. Furthermore, in cases where a transmural perfusion defect was observed concomitant to a coronary stenosis, it was considered a true perfusion defect regardless of the potential presence of an underlying BHA.

SPECT analysis was carried out by consensus of two experienced observers (R.C. and M.L.M.) blinded to the CT data. For this purpose, reconstruction into long- and short-axis projections perpendicular to the heart axis was initially performed, followed by an automated quantitative analysis of the perfusion images using polar map format (normalized to 100%). Myocardial perfusion defects were identified as segmental tracer activity less than 75% of maximum. Gated images were used to assess regional wall motion to enhance the discrimination between perfusion defects and attenuation artifacts.

CT effective radiation dose was derived by multiplying the dose-length product with the weighting (k) value of 0.014 mSv/mGy/cm for chest examinations, as suggested by the Society of Cardiovascular Computed Tomography (9). Radiation dosimetry of SPECT was estimated based on the recommendations of recently published guidelines.(12).

The institution's Ethics Committee approved the study protocol, which complied with the Declaration of Helsinki, and written informed consent was obtained from all patients.

Statistical Analysis

Discrete variables are presented as counts and percentages. Continuous variables are presented as means ± standard deviation. Comparisons among groups were performed using independent samples t test. The agreement between observers was tested using Kappa coefficient. To determine the accuracy of CT perfusion for the detection of perfusion defects by SPECT, we calculated the sensitivity, specificity, negative predictive value, positive predictive value, likelihood ratios, and

diagnostic odds ratios accounting for potential nonuniform distribution (95% confidence intervals). ROC curve analyses were also performed to evaluate the diagnostic performance of the two diagnostic approaches using specific software for ROC analysis (MedCalc Software, Ostend, Belgium). The difference between the two areas under the curve (AUCs) was tested with the z test. Differences in the parameters a and b of two ROC curves are tested using the bivariate chi-square test, as previously described (13,14). For comparison between independent sample ROC curves the Hanley method based on the standard error was used (15). All other statistical analyses were performed using SPSS software, version 13.0 (SPSS Inc, Chicago, Illinois). A two-sided P value of less than 0.05 indicated statistical significance.

RESULTS

Forty patients were prospectively and sequentially included in the study protocol (the first 20 using DECT and the second 20 using SECT). The mean age was 60.1 ± 9.4 years. Twenty-nine (72.5%) patients were male. Ten patients (25%) had diabetes, 34 had hypertension (85%), and 33 had hypercholesterolemia (83%). The demographic characteristics did not differ between groups. Indeed, no significant differences were observed regarding the body mass index (DECT 27.8 ± 3.9 kg/m^2 vs. SECT 27.9 ± 4.0 kg/m^2; P = .67) or the heart rate 1 hour before the CT scan (DECT 63.3 ± 6.5 bpm vs. SECT 60.5 ± 6.5 bpm; P = .20). Most patients were receiving baseline beta-blockers, with no differences between groups (DECT n = 17 [85%], SECT n = 17 [85%]). The mean estimated pretest likelihood of obstructive CAD (Duke) was 69.1 ± 23.5% for the DECT group and 72.2 ± 21.5% for the SECT group (P = .67).

Image Quality and Effective Radiation Dose

Both the myocardial SD ratio (DECT 0.31 ± 0.07 vs. SECT 0.31 ± 0.07; P = .99) and the contrast-to-noise ratio (DECT 8.8 ± 2.9 vs. SECT 7.7 ± 4.2; P = .22) were similar between groups. Nevertheless, DECT showed higher contrast-to-noise ratio than SECT among stress scans (Fig 1). Conversely, among rest scans, SECT showed a trend toward higher contrast-to-noise ratio compared to DECT (Fig 1).

The mean effective radiation dose was 7.4 ± 1.1 mSv with DECT and 9.9 ± 3.8 mSv with SECT (P = .011). Radiation dose of SPECT imaging was 8.8 ± 2.0 mSv. Table 1 shows discriminated radiation doses.

Diagnostic Performance of DECT Versus SECT

A total of 1360 left ventricular segments were evaluated by DECT and SECT (Figs 2–4). Among the DECT group, two (0.29%) segments were deemed nonassessable because of motion artifacts and considered positive as prespecified in the study protocol, whereas all segments were evaluable

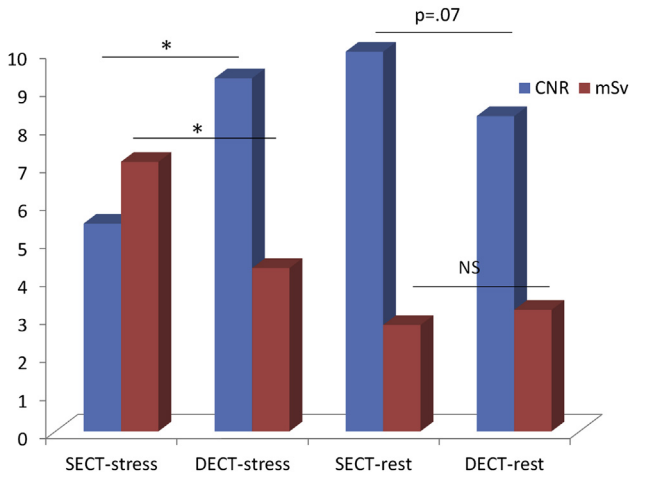

Figure 1. Bar graph comparing image quality (contrast-to-noise ratio, CNR) and effective radiation dose (mSv) among dual-energy computed tomography (DECT) and single-energy computed tomography (SECT) both at stress and rest. NS, non-significant.
*p < 0.05.

TABLE 1. Effective Radiation Doses

	Radiation Dose (mSV)			*P* Value SPECT vs.	
Scan	DECT	SECT	SPECT	DECT	SECT
Stress	4.3 ± 1.0	7.1 ± 2.6*			
Rest	3.2 ± 0.4	2.8 ± 2.1†			
Total	7.4 ± 1.1	9.9 ± 3.8‡	8.8 ± 2.0	0.06	0.41

DECT, dual-energy computed tomography; SECT, single-energy computed tomography; SPECT, single-photon emission computed tomography.
*P < .001 versus DECT.
†Nonsignificant differences versus DECT.
‡P < .05 versus DECT.

with SECT. The sensitivity, specificity, positive predictive value, and negative predictive value of DECT for detection of myocardial perfusion defects were 84.1% (76.3%–89.8%), 96.4% (94.4%–97.7%), 84.1% (76.3%–89.8%), and 96.4% (94.4%–97.7%), respectively.

With regard to SECT, the sensitivity, specificity, positive predictive value, and negative predictive value for detection of myocardial perfusion defects were 69.1% (62.7%–74.5%), 91.3% (88.2%–93.6%), 80.5% (74.2%–85.6%), and 85.0% (81.4%–88.0%), respectively.

The positive likelihood ratio was 23.3 (15.1–36.1) for DECT and 7.9 (5.8–10.8) for SECT, whereas the negative likelihood ratio was 0.16 (0.11–0.25) for DECT and 0.34 (0.28–0.41) for SECT. The diagnostic odds ratio was 141.5 (73.6–272.1) for DECT and 23.7 (15.4–36.5) for SECT.

The diagnostic performance of DECT was greater than that of SECT in identifying perfusion defects (AUC of DECT 0.90 [0.86–0.94] vs. SECT 0.80 [0.76–0.84]; P = .0004).

Finally, there was a good agreement between observers for the presence of myocardial perfusion defects evaluated by DECT (kappa = 0.89, P < .001).

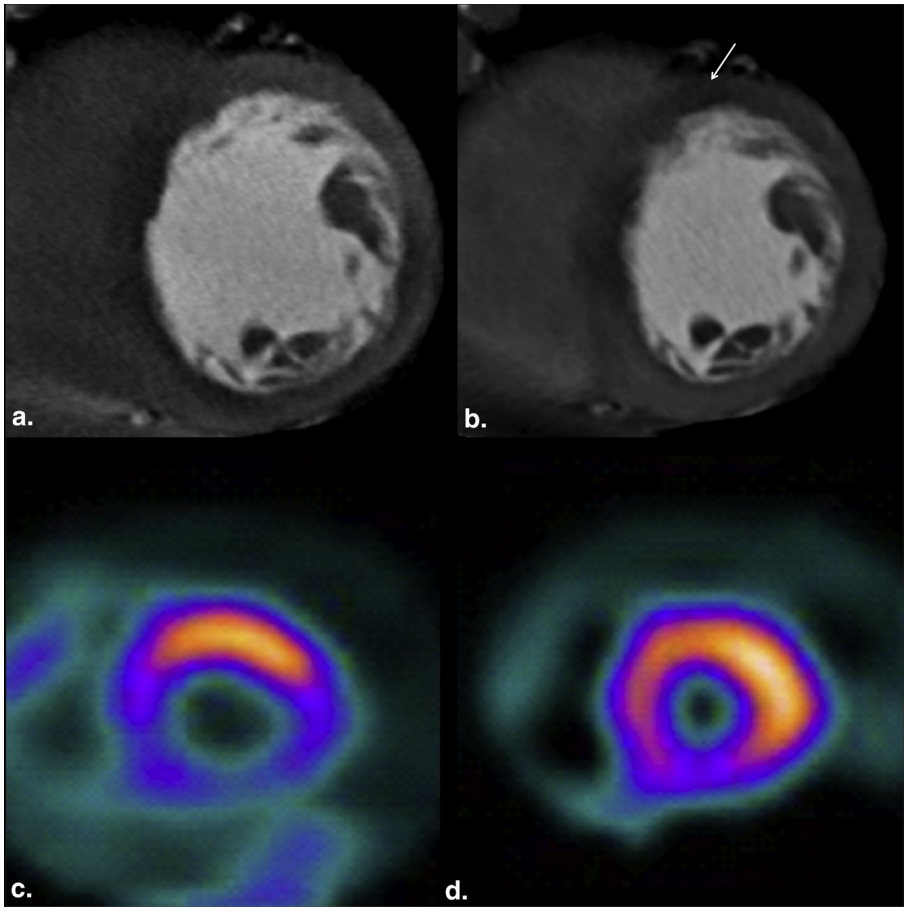

Figure 2. Example of beam-hardening artifact (BHA) with single-energy computed tomography (SECT). Stress (*panels* **a** and **c**) and rest (*panels* **b** and **d**) short-axis views of SECT (*above*) and single-photon emission computed tomography (SPECT, *below*). Inferior and inferoseptal wall reversible defect (ischemia) is observed with both approaches. A BHA can be recognized as a significant myocardial signal density drop resembling a perfusion defect at the anterior wall in rest (*arrow*), with normal perfusion both at stress and with SPECT.

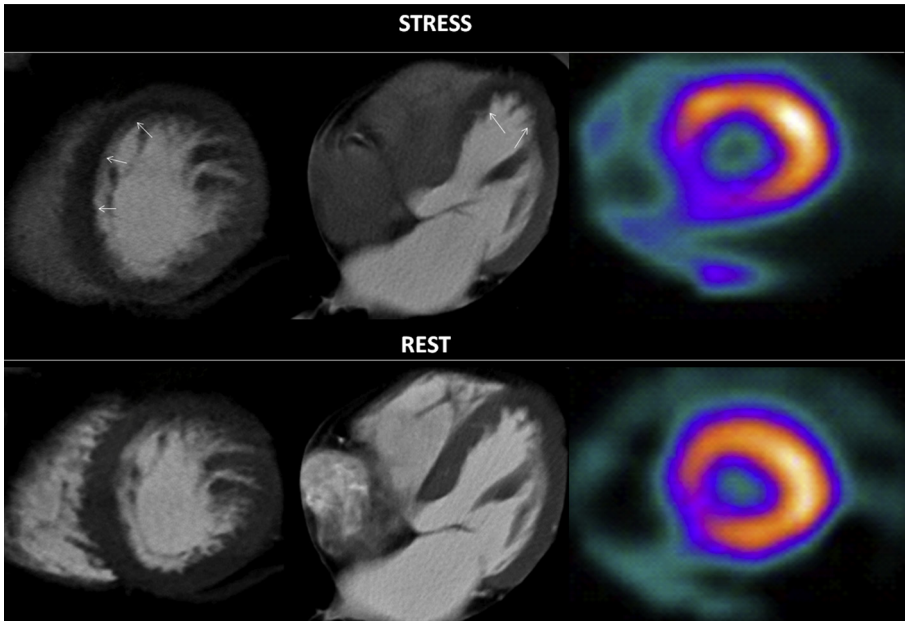

Figure 3. Myocardial perfusion imaging by single-energy computed tomography (SECT) in a 61-year-old male with hypercholesterolemia and previous smoking as coronary risk factors, and chest pain, referred for myocardial perfusion imaging by single-photon emission computed tomography (SPECT). *Above*: stress images of SECT in a short-axis apical view (*left panel*) and a four-chamber view (*center panel*), and SPECT imaging in a short-axis apical view (*right panel*). *Below*: corresponding rest images. SECT imaging demonstrates a perfusion defect (*arrows*) during stress in the septal and apical wall of the left ventricle, with normalization of myocardial perfusion in rest.

On the per-patient analysis, the sensitivity, specificity, positive predictive value, and negative predictive value of SECT for detection of myocardial perfusion defects were 100% (80.5%–100%), 100% (29.2%–100%), 100% (80.5%–100%), and 100% (29.2%–100%), respectively, whereas DECT values were 100% (73.2%–100%), 83.3% (36.5%–99.1%), 93.3% (66.0%–100%), and 100% (46.3%–100%). It should be noted that the single false positive of DECT on a per-patient basis

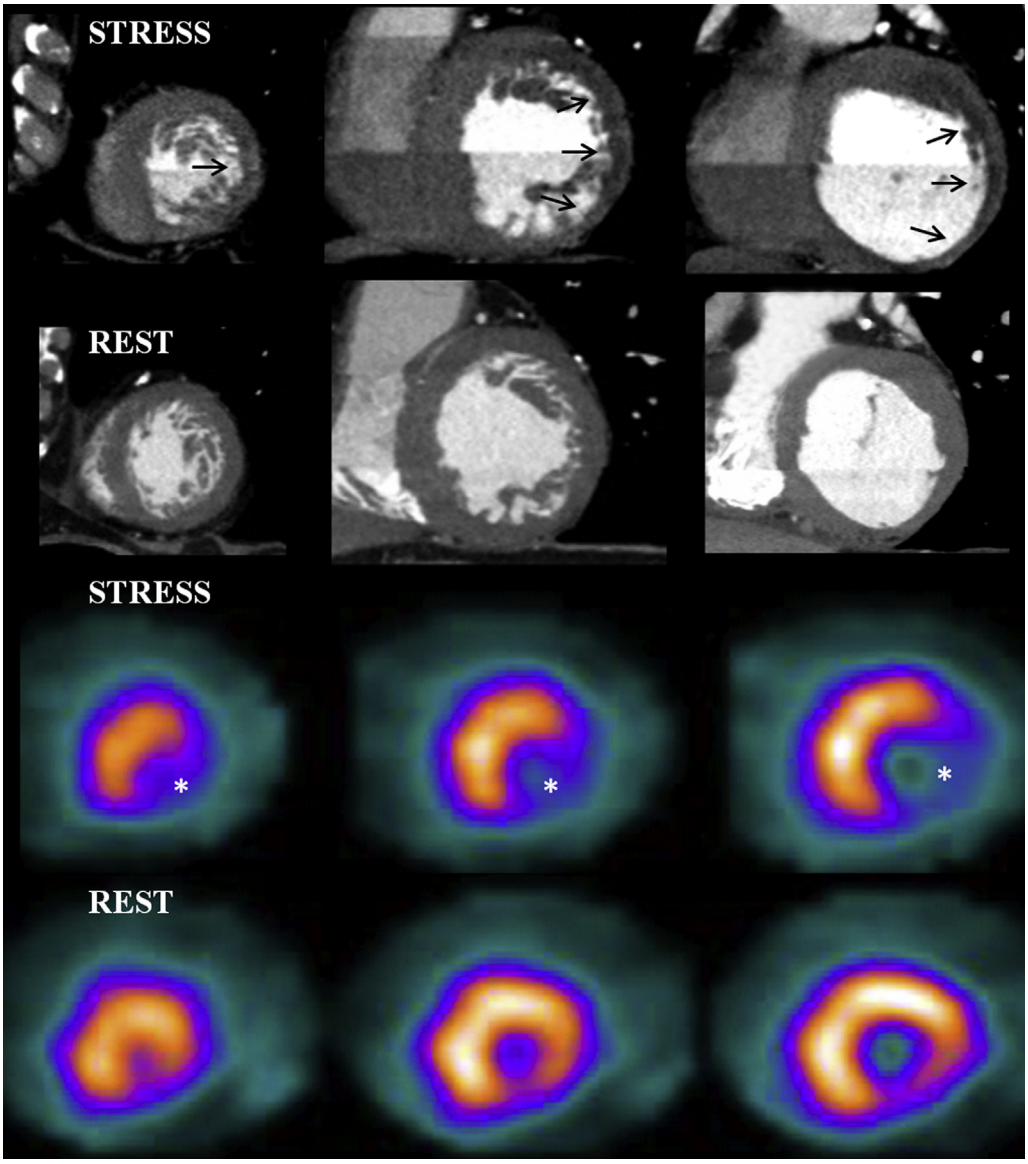

Figure 4. Myocardial perfusion imaging by dual-energy computed tomography (DECT) in a 79-year-old male with hypertension and hypercholesterolemia as coronary risk factors, and chest pain, referred for myocardial perfusion imaging by single-photon emission computed tomography (SPECT). Apical (*left*), mid ventricular (*center*), and basal (*right*) short-axis views of DECT (*above*) and SPECT (*below*) both at stress and rest. DECT imaging demonstrates a perfusion defect (*arrows*) during stress in the anterolateral and inferolateral wall, with normalization of myocardial perfusion in rest and good correlation with the perfusion defect observed at SPECT (*).

was attributed to a single segment (segment #14) and only observed in rest (Table 2).

Analysis Including Segments Affected by BHAs

When including only segments commonly affected by BHAs (Fig 2), the sensitivity, specificity, positive predictive value, and negative predictive value of DECT were 86.6% (71.9%–94.3%), 93.6% (88.2%–96.7%), 79.2% (64.6%–89.0%), and 96.1% (91.2%–98.4%), respectively, with a positive likelihood ratio of 13.5 (7.3–24.8) and a negative likelihood ratio of 0.15 (0.07–0.31). In parallel, SECT analysis of such segments yielded a sensitivity, specificity, positive predictive value, and negative predictive value of 69.1% (56.6%–79.5%), 84.1% (76.5%–89.7%), 69.1% (56.6%–79.5%), and 84.1% (76.5%–89.7%), respectively, with a positive likelihood ratio of 4.3 (2.8–6.6) and a negative likelihood ratio of 0.37 (0.26–0.52).

Among BHA segments, the diagnostic performance of DECT was greater than that of SECT in identifying perfusion defects (AUC of DECT 0.90 [0.84–0.96] vs. SECT 0.77 [0.69–0.84]; $P = .007$). Furthermore, *post hoc* analysis including only segments without BHA revealed no

TABLE 2. Diagnostic Performance of SECT and DECT

Diagnostic performance	SECT	DECT	SECT BHA	DECT BHA
Sensitivity (%)	70.3 (63.9–76.1)	82.8 (75.1–88.9)	69.1 (56.6–79.5)	86.6 (71.9–94.3)
Specificity (%)	90.7 (87.6–93.2)	96.7 (94.9–98.1)	84.1 (76.5–89.7)	93.6 (88.2–96.7)
Positive predictive value (%)	79.3 (73.0–84.7)	85.5 (78.0–91.2)	69.1 (56.6–79.5)	79.2 (64.6–89.0)
Negative predictive value (%)	85.7 (82.2–88.7)	96.0 (94.1–97.5)	84.1 (76.5–89.7)	96.1 (91.2–98.4)
Positive likelihood ratio	7.5 (5.6–10.2)	25.4 (16.1–40.2)	4.3 (2.8–6.6)	13.5 (7.3–24.8)
Negative likelihood ratio	0.33 (0.27–0.40)	0.18 (0.12–0.25)	0.37 (0.26–0.52)	0.15 (0.07–0.31)
Diagnostic odds ratio	23.1 (14.8–36.2)	142.9 (70.9–291.7)	11.8 (5.9–23.7)	92.5 (31.6–270.4)
Area under the curve (ROC)	0.80 (0.76–0.84)	0.90 (0.86–0.94)	0.77 (0.69–0.84)	0.90 (0.84–0.96)

BHA, beam-hardening artifact; DECT, dual-energy computed tomography; ROC, receiver operating characteristic; SECT, single-energy computed tomography.

significant differences between DECT and SECT regarding the detection of perfusion defects (AUC of DECT 0.90 [standard error 0.03] vs. SECT 0.82 [standard error 0.06]; $P = .20$).

DISCUSSION

Our results suggest that myocardial perfusion by DECT imaging is feasible and might have improved diagnostic performance compared to SECT imaging for the assessment of myocardial CT perfusion, preserving image quality and without increment in effective radiation dose levels. Furthermore, the diagnostic performance of DECT remained unaffected by the presence of BHAs.

During the past decade, CCTA main limitation is the inability to predict the functional significance of coronary stenosis because of its low positive predictive value in patients with high likelihood of CAD, mainly attributed to overestimation of stenosis in the presence of calcified plaques. Several studies reported the ability to acquire stress myocardial CT perfusion to overcome this challenge, although with the limitation of BHA (Fig 2) (16,17). Meijboom et al. confirmed these limitations in a study where they reported that CCTA does not provide additional relevant diagnostic information in symptomatic patients with a high estimated pretest probability of CAD (16,17).

Assessment of the hemodynamic significance of intermediate lesions is pivotal because deferring revascularization of stenotic lesions that do not cause ischemia is safe and associated with very low rates of death or myocardial infarction (18,19). In line with the limitations of conventional angiography itself, the anatomic evaluation of the hemodynamic significance of coronary stenoses by CCTA is only moderately correlated with the functional assessment by fractional flow reserve, being this more evident in the presence of diffusely calcified vessels that often lead to false-positive results and therefore suboptimal positive predictive values (20,21). Overall, these reasons have lead to the exclusion of CCTA from diagnostic algorithms of patients with high pretest probability of CAD or in the elderly. Accordingly, significant efforts and different strategies have been proposed to attempt a simultaneous assessment of both coronary anatomy and myocardial perfusion (1,2,20–22).

Nevertheless, conventional CT (SECT) is limited to some extent for myocardial perfusion imaging mainly by the presence of BHAs that commonly affect two coronary territories and is independent of body mass index, blood SD of the left and right ventricles, contrast-to-noise ratio, and the extent of atherosclerosis (5). In contrast, by allowing simulated monochromatic image reconstruction, DECT imaging has evolved during the past few years as a promising technique with the potential to significantly reduce BHA.

There are essentially two approaches to evaluate myocardial perfusion with DECT: source-oriented or detector-oriented approach. The source-oriented approach is the most widely studied and is based on a CT scanner equipped with two independent x-ray tubes and a set of detectors at an angular offset of 90–94°, with one tube operating at 80 or 100 kV and the other operating at 140 kV (23). The detector-oriented approach that we hereby describe comprises a CT scanner with a single x-ray tube capable of rapid switching between 80 and 140 kV, hence shows promise to overcome some limitations of the source-oriented approach, such as increased scattered radiation and potential mismatch in the projection views between the high and low tube projections when scanning moving objects such as the heart.

To the best of our knowledge, this is the first prospective study to compare the diagnostic performance of DECT using gemstone detectors for spectral imaging versus SECT to evaluate stress myocardial perfusion. In this pilot investigation, where two contemporary state of the art CT systems were compared, we have demonstrated that DECT allows an accurate evaluation of stress myocardial perfusion in patients with intermediate to high likelihood of CAD and appears to unravel one of the main limitations of SECT imaging, the presence of BHAs. In fact, the diagnostic performance of DECT remained unaffected when including only the segments commonly affected by BHA.

Furthermore, DECT, a prospective acquisition *per se*, was associated with a significant reduction (approximately 15%) in radiation dose with respect to SECT, a difference mainly attributed to stress imaging, scenario where SECT requires

retrospective gating because of the increase in heart rate observed during pharmacologic stress. Nevertheless, it is noteworthy that even SECT imaging (stress plus rest) was related to similar overall radiation dose than SPECT, being important to underscore the fact that a comprehensive assessment of both anatomy and function can be performed at the expense of less than 10 mSv. Among single energy acquisitions, the stress scan was performed using retrospective gating to obtain systolic and diastolic phases aimed at obtaining optimal myocardial perfusion evaluation even in the presence of high heart rates. Rest scan was acquired using prospective gating. It should be noted that prospective acquisitions in stress imaging are associated with longer acquisition times, potentially leading to related artifacts.

The relative low radiation dose of DECT imaging (~7–8 mSv) should be put into perspective against the recently reported higher radiation exposure with dynamic CT perfusion (~13 mSv) (2). It should be emphasized however, that DECT radiation exposure could have been lower because ECG padding (additional surrounding x-ray beam over time that results in supplementary available phases for analysis) has been associated with a significant increase in radiation doses (24,25). Notwithstanding, we decided to use padding in DECT to ensure image quality in a developing technology, whereas rest myocardial perfusion imaging in SECT patients was performed without padding.

Although the usefulness of CCTA remains focused on patients with low to intermediate likelihood of CAD, our findings could potentially provide preliminary groundwork for potential expansion of the clinical applications of CCTA to patients with intermediate to high likelihood of CAD.

Limitations

A number of limitations should be acknowledged. The relatively small sample size might lead to selection bias. Furthermore, invasive angiography with fractional flow reserve was not performed to confirm the presence of obstructive CAD; therefore, the reference standard (SPECT) is potentially subject to error. The primary end point of the study was to explore the feasibility and diagnostic performance of DECT versus SECT regarding myocardial perfusion; therefore, data regarding the incremental value of coronary anatomy over myocardial perfusion in DECT will be prospectively investigated in further studies. ROC analysis based on segmental analyses might be partially affected by the lack of independence within a single patient. We also acknowledge that the most appropriate means to compare the diagnostic performance of the two methods would have been to perform both approaches on the same patients. Nevertheless, because of obvious ethical grounds and to restrictions of the Institutional Ethics Committee, we decided to enroll two consecutive cohorts of patients. Finally, randomization was not performed because the CT scanners are localized at different sites (of the same Institution).

CONCLUSIONS

In this pilot investigation, myocardial perfusion assessment by DECT imaging in patients with intermediate to high likelihood of CAD was feasible and remained unaffected by the presence of BHAs. Furthermore, DECT showed a higher diagnostic performance than SECT imaging, although these encouraging findings should be considered with caution given the relatively small sample size and the selected patient population.

REFERENCES

1. Ko BS, Cameron JD, Leung M, et al. Combined CT coronary angiography and stress myocardial perfusion imaging for hemodynamically significant stenoses in patients with suspected coronary artery disease: a comparison with fractional flow reserve. JACC Cardiovasc Imaging 2012; 5: 1097–1111.
2. Bamberg F, Becker A, Schwarz F, et al. Detection of hemodynamically significant coronary artery stenosis: incremental diagnostic value of dynamic CT-based myocardial perfusion imaging. Radiology 2011; 260:689–698.
3. Rocha-Filho JA, Blankstein R, Shturman LD, et al. Incremental value of adenosine-induced stress myocardial perfusion imaging with dual-source CT at cardiac CT angiography. Radiology 2010; 254:410–419.
4. Ko SM, Choi JW, Hwang HK, et al. Diagnostic performance of combined noninvasive anatomic and functional assessment with dual-source CT and adenosine-induced stress dual-energy CT for detection of significant coronary stenosis. AJR Am J Roentgenol 2012; 198:512–520.
5. Rodríguez-Granillo GA, Rosales MA, Degrossi E, et al. Signal density of left ventricular myocardial segments and impact of beam hardening artifact: implications for myocardial perfusion assessment by multidetector CT coronary angiography. Int J Cardiovasc Imaging 2010; 26:345–354.
6. So A, Lee TY, Imai Y, et al. Quantitative myocardial perfusion imaging using rapid kVp switch dual-energy CT: preliminary experience. J Cardiovasc Comput Tomogr 2011; 5:430–442.
7. Gibbons RJ, Balady GJ, Bricker JT, et al. American College of Cardiology/American Heart Association Task Force on Practice Guidelines. Committee to Update the 1997 Exercise Testing Guidelines. ACC/AHA 2002 guideline update for exercise testing: summary article. A report of the American College of Cardiology/American Heart Association Task Force on Practice Guidelines (Committee to Update the 1997 Exercise Testing Guidelines). J Am Coll Cardiol 2002; 40:1531–1540.
8. Pryor DB, Shaw L, McCants CB, et al. Value of the history and physical in identifying patients at increased risk for CAD. Ann Intern Med 1993; 118: 81–90.
9. Halliburton SS, Abbara S, Chen MY, et al. Society of Cardiovascular Computed Tomography. SCCT guidelines on radiation dose and dose-optimization strategies in cardiovascular CT. J Cardiovasc Comput Tomogr 2011; 5:198–224.
10. Carrascosa P, Rodriguez-Granillo GA, Capunay C, et al. Low-dose CT coronary angiography using iterative reconstruction with a 256-slice CT scanner. World J Cardiol 2013; 5:382–386.
11. Cerqueira MD, Weissman NJ, Dilsizian V, et al. American Heart Association Writing Group on Myocardial Segmentation and Registration for Cardiac Imaging. Standardized myocardial segmentation and nomenclature for tomographic imaging of the heart: a statement for healthcare professionals from the Cardiac Imaging Committee of the Council on Clinical Cardiology of the American Heart Association. Circulation 2002; 105: 539–542.
12. Dorbala S, Di Carli MF, Delbeke D, et al. SNMMI/ASNC/SCCT Guideline for Cardiac SPECT/CT and PET/CT 1.0. J Nucl Med 2013; 54:1485–1507. http://dx.doi.org/10.2967/jnumed.112.105155.
13. Park SH, Goo JM, Jo CH. Receiver operating characteristic (ROC) curve: practical review for radiologists. Korean J Radiol 2004; 5:11–18.
14. Metz CE. Some practical issues of experimental design and data analysis in radiologic ROC studies. Invest Radiol 1989; 24:234–245.
15. Hanley JA, McNeil BJ. The meaning and use of the area under a receiver operating characteristic (ROC) curve. Radiology 1982; 143:29–36.
16. Arbab-Zadeh A, Miller JM, Rochitte CE, et al. Diagnostic accuracy of computed tomography coronary angiography according to pre-test

probability of coronary artery disease and severity of coronary arterial calcification. The CORE-64 (Coronary Artery Evaluation Using 64-Row Multidetector Computed Tomography Angiography) International Multicenter Study. J Am Coll Cardiol 2012; 59:379–387.
17. Meijboom WB, van Mieghem CAG, Mollet NR, et al. 64-Slice computed tomography coronary angiography in patients with high, intermediate, or low pretest probability of significant coronary artery disease. J Am Coll Cardiol 2007; 50:1469–1475.
18. Pijls NH, van Schaardenburgh P, Manoharan G, et al. Percutaneous coronary intervention of functionally nonsignificant stenosis: 5-year follow-up of the DEFER Study. J Am Coll Cardiol 2007; 49: 2105–2111.
19. Tonino PA, De Bruyne B, Pijls NH, et al. FAME Study Investigators. Fractional flow reserve versus angiography for guiding percutaneous coronary intervention. N Engl J Med 2009; 360:213–224.
20. Meijboom WB, Van Mieghem CA, van Pelt N, et al. Comprehensive assessment of coronary artery stenoses: computed tomography coronary angiography versus conventional coronary angiography and correlation with fractional flow reserve in patients with stable angina. J Am Coll Cardiol 2008; 52:636–643.
21. Rodríguez-Granillo GA, Ingino CA, Lylyk P. Myocardial perfusion imaging and infarct characterization using multidetector cardiac computed tomography. World J Cardiol 2010; 2:198–204.
22. Yoon YE, Choi JH, Kim JH, et al. Noninvasive diagnosis of ischemia-causing coronary stenosis using CT angiography: diagnostic value of transluminal attenuation gradient and fractional flow reserve computed from coronary CT angiography compared to invasively measured fractional flow reserve. JACC Cardiovasc Imaging 2012; 5:1088–1096.
23. Arnoldi E, Lee YS, Ruzsics B, et al. CT detection of myocardial blood volume deficits: dual-energy CT compared with single-energy CT spectra. J Cardiovasc Comput Tomogr 2011; 5:421–429.
24. Min JK, Leipsic J, Pencina MJ, et al. Diagnostic accuracy of fractional flow reserve from anatomic CT angiography. JAMA 2012; 308:1237–1245.
25. Labounty TM, Leipsic J, Min JK, et al. Effect of padding duration on radiation dose and image interpretation in prospectively ECG-triggered coronary CT angiography. AJR Am J Roentgenol 2010; 194:933–937.